ELSEVIER

Journal of Wind Engineering
and Industrial Aerodynamics 92 (2004) 789–804

JOURNAL OF wind engineering AND industrial aerodynamics

www.elsevier.com/locate/jweia

Efficient models for wind turbine extreme loads using inverse reliability

K. Saranyasoontorn, L. Manuel*

Department of Civil Engineering, University of Texas at Austin, 1 University Station, C1748, Austin, TX 78712, USA

Received 8 December 2003; received in revised form 20 January 2004; accepted 14 April 2004

Abstract

The reliability of wind turbines against extreme loads is the focus of this study. A procedure to establish nominal loads for use in a conventional load-and-resistance-factor-design format is presented. The procedure, based on an inverse reliability approach, permits inclusion of randomness in the gross wind environment as well as in the extreme response given wind conditions. A detailed example is presented where three alternative nominal load definitions are used to estimate extreme bending loads for a 600 kW three-bladed horizontal-axis wind turbine. Only operating loads—here, flapwise (out-of-plane) bending moments—at a blade root are considered but the procedure described may be applied to estimate other loads and response measures of interest in wind turbine design. Results suggest that a full random characterization of both wind conditions and short-term maximum response (given wind conditions) will yield extreme design loads that might be approximated reasonably well by simpler models that include only the randomness in the wind environment but that account for response variability by employing appropriately derived "higher-than-median" fractiles of the extreme bending load conditional on inflow parameter values.

Keywords: Wind turbine; Reliability; Extreme load; Flapwise bending moment

1. Introduction

In reliability-based design, the conventional load-and-resistance-factor-design (LRFD) procedure involves the scaling of a nominal load, L_{nom}, by a load factor, γ_{L},

*Corresponding author. Tel.: +1-512-232-5691; fax: +1-512-471-7259.
E-mail addresses: korn.ae@mail.utexas.edu (K. Saranyasoontorn), lmanuel@mail.utexas.edu (L. Manuel).

0167-6105/$ - see front matter © 2004 Elsevier Ltd. All rights reserved.
doi:10.1016/j.jweia.2004.04.002

and the scaling of a nominal (or characteristic) resistance, R_{nom}, by a separate resistance factor, ϕ_{R}, to account for possible overload and understrength. This is done in the following checking equation which aims to provide for design against a specified limit state:

$$\phi_{\text{R}} R_{\text{nom}} \geqslant \gamma_{\text{L}} L_{\text{nom}}. \tag{1}$$

Calibration of both the scaling factors and the associated definitions of L_{nom} (for example, as a load level associated with a specified return period) and R_{nom} are needed to guarantee specified probabilities of meeting the limit state under consideration. For wind turbine generator systems, a similar reliability-based design format is employed in the IEC 61400-1 code where the load factor, γ_{L}, and the resistance factor, ϕ_{R}, in Eq. (1) are combined into a single factor, γ_{n}, that represents a safety factor for "consequences of failure" [1].

Various alternative definitions of the nominal load level may be employed to account for load variability. In the present study for wind turbine extreme loads, we consider three such load definitions related to assumptions used in representing load uncertainty in Eq. (1). The key uncertainties in the design of wind turbines arise from (i) the gross inflow parameters, usually taken to be the 10-min mean horizontal wind speed at hub height and the standard deviation (also a measure of turbulence intensity) of the same wind speed process; and (ii) the 10-min maximum load/response conditional on the inflow parameters.

In the following, we refer to the inflow parameters as simply mean and standard deviation of wind speed, with an understanding that we are referring to statistics of the time-varying horizontal wind speed process at hub height. We consider an extreme flapwise (out-of-plane) bending moment at the blade root as the load of interest. Our objective is to establish appropriate nominal design loads for several target reliability levels (or, equivalently, for several different return periods). These loads defined with different degrees of complexity in the assumptions on the variability of the key random variables are compared and insights gained from this comparison are discussed to aid in development of a rational procedure for establishing design loads.

2. Structural reliability and inverse methods

The first-order reliability method (FORM) is essentially an "analysis" approach whereby one seeks a "solution" which corresponds to a most-likely-to-fail combination of the various load and resistance quantities (for details related to FORM, see [2]). The probability of failure associated with this combination is easily estimated but it is not known a priori. An iterative approach in such "forward-FORM" analyses where one adjusts, for example, the resistance/capacity level to yield a specified reliability or probability of failure would constitute a "design" procedure. This iterative procedure, however, is tedious in many situations.

An alternative approach is to use "inverse reliability" techniques that avoid multiple forward-FORM iterations. Many recent studies have proposed procedures

for these techniques and/or have applied them to different design problems. Winterstein et al. [3] developed an inverse first-order reliability method (inverse-FORM) procedure that is based on the use of "environmental contours" that uncouple environmental random variables from structural response. Using examples related to offshore structures, they showed how this method may be applied to estimate design loads associated with specified target reliability levels. Der Kiureghian et al. [4] proposed an extension of the Hasofer–Lind–Rackwitz–Fiessler FORM algorithm that uses a search direction and a merit function as part of a very efficient procedure that finds the design point associated with a target reliability. Li and Foschi [5] showed, using several examples, how multiple design variables may be treated in an inverse reliability procedure.

Recently, Fitzwater et al. [6] applied inverse reliability methods for extreme loads on pitch- and stall-regulated wind turbines where they employed results from aeroelastic simulations to represent the response given inflow conditions. The response variable there was treated as deterministic allowing the use of 2-D environmental contours based on Winterstein et al. [3]. In the present study, our interest is in estimating design extreme flapwise bending loads for a 600 kW three-bladed horizontal-axis wind turbine that was previously studied by Ronold and Larsen [7], where results from field measurements were reported and probabilistic models for response (loads) conditional on inflow conditions were presented. The distinction between the present study and that by Fitzwater et al. [6] is that we propose alternative nominal load definitions (one of which includes response variability) and we employ field data instead of simulations in developing parametric models for the random response conditional on inflow. Our alternative load definitions are based on what will be described as 1-D, 2-D, and 3-D models which refer to how the inflow and response variables are treated—i.e., whether deterministic or random. The full 3-D characterization of variables refers to modeling of all variables as random, while the other two models refer to simplifications where, in the 1-D case, only mean wind speed is modeled as random and, in the 2-D case, the mean and standard deviation of the wind speed are both modeled as random (but response is not). A discussion of enhancements to the 2-D model that reflect omitted randomness in the response (conditional on inflow) is presented that is based on the use of omission sensitivity factors [8,3]. Such enhancements approximately get at the full randomness of the response by employing "higher-than-median" fractiles of the extreme bending load conditional on inflow—these are improvements on the ordinary 2-D model that uses a deterministic representation of response or, effectively, median levels of load conditional on inflow.

The alternative nominal load definitions are presented next, along with a general background on the Inverse-FORM framework for establishing design loads. Design load levels for different return periods based on the alternative models are compared for the 600 kW wind turbine described by Ronold and Larsen [7].

3. Alternative models

Our interest here is in obtaining estimates of a nominal load, L_{nom}, for failure in an extreme/ultimate limit state associated with bending of a wind turbine blade in its flapwise (out-of-plane) mode. We assume that the uncertainty in these extreme bending loads depends on inflow parameters and on short-term maximum loads conditional on the inflow parameters. As stated previously, the inflow parameters that characterize the wind are the ten-minute mean wind speed at hub height, U_{10}, and the standard deviation, σ, of the wind speed. The load, L_{nom}, considered here is the extreme flapwise bending moment at the root of a turbine blade corresponding to a specified return period of T years. From the field data on the wind turbine considered, ten-minute extremes of the random flapwise bending moment, M_{ext}, are used to derive the nominal load, L_{nom}. For convenience, in discussions that follow, we will refer to the three short-term (i.e., 10-min) random variables, U_{10}, σ, and M_{ext} as X_1, X_2, and X_3 that make up the physical random variable space, $\boldsymbol{X}$.

Consider a situation where the joint probability description of X_1, X_2, and X_3 is available in the form of a marginal distribution for X_1 and conditional distributions for X_2 given X_1, and for X_3 given X_1 and X_2. The simplest definition of L_{nom} is based on a representative load derived from the T-year value of the random X_1 (mean wind speed) alone and consideration of X_2 (standard deviation on wind speed) and X_3 (10-min extreme bending load) only by representing these as conditional median values. In this model for L_{nom}, uncertainty is neglected in both X_2 and X_3. A second definition might be based on a representative T-year load that includes randomness in both X_1 and X_2 but still neglects uncertainty in the short-term load, X_3. Again, this load is held fixed at its median level given X_1 and X_2. Finally, a definition for nominal load could be based on the "true" T-year nominal load including uncertainty in all of the three variables. We refer to these definitions as "1-D", "2-D", and "3-D" probabilistic models, respectively. The nominal loads based on these models can be expressed as

$$\begin{aligned} L_{\text{nom,1-D}} &= \hat{X}_3(X_1, \hat{X}_2|X_1),\ L_{\text{nom,2-D}} = \hat{X}_3(X_1, X_2|X_1), \\ L_{\text{nom,3-D}} &= X_3(X_1, X_2|X_1) \end{aligned} \tag{2}$$

in which $\hat{X}_2$ represents the median of X_2, $\hat{X}_3$ denotes the median of X_3, and "|" denotes a conditional sign (for example, $\hat{X}_2|X_1$ refers to the median value of X_2 given X_1). The load factor, γ_L, in Eq. (1) will be appropriately different for each of the nominal load definitions above in order to ensure that the design checking equation leads to consistent reliability estimates in each case. In the following, we use an example wind turbine and available field data, and then derive and compare nominal wind turbine bending loads based on these three probabilistic models.

It is possible to establish nominal loads by direct integration involving the conditional short-term maximum load distribution (given inflow conditions) and the joint density function of the inflow variables. For the right choice of L_{nom},

integration will lead to the desired target probability of failure, P_f, as follows:

$$P_f = P[X_3 > L_{nom}] = \int\int_{X_1,X_2} P[X_3 > L_{nom}|X_1, X_2] f_{X_1,X_2}(x_1, x_2)\, dx_1\, dx_2, \quad (3)$$

where $f_{X_1,X_2}(x_1, x_2)$ is the joint probability density function of X_1 and X_2. Using Eq. (3) to obtain the nominal load would provide the "exact" load but would be computationally expensive in practical situations. Also, not much would be learned about the inflow conditions that bring about this load. Inverse reliability procedures, on the other hand, are approximate but less computationally intensive and have an important advantage in that they offer useful insights into the derived load and about the associated inflow conditions. In particular, we will use the Inverse-FORM approach proposed by Winterstein et al. [3]. An overview is presented next of how this method based on environmental contours works in the current study.

Consider a sphere of radius equal to the target reliability index, β, in an n-dimensional space describing independent standard normal variables, one for each of the physical random variables in the problem of interest. If at any point on this sphere, a tangent hyperplane were drawn, the probability of occurrence of points on the side of this hyperplane away from the origin is $\Phi(-\beta)$, where $\Phi(\,)$ refers to the Gaussian cumulative distribution function. Since each point on the sphere is associated with the same reliability level, if the nominal load desired is also for this same level, the points on the sphere can be systematically searched until the largest nominal load is obtained. Transformation from the standard normal ($\boldsymbol{U}$) space to the physical random variable ($\boldsymbol{X}$) space is necessary in order to obtain the nominal load. This is achieved by using the Rosenblatt transformation [9]. In the present study, a complete probabilistic representation of the random variables requires that n is equal to 3. However, we shall see how only the 3-D model in Eq. (2) retains all three random variables. The median value indicated in the definition of $L_{nom,2\text{-}D}$ in Eq. (2) is equivalent to forcing the variable U_3 to be zero; and for $L_{nom,1\text{-}D}$, it is equivalent to forcing the two variables, U_2 and U_3 to both be zero. This has the effect of causing 2-D and 1-D models for L_{nom} to be obtained by reducing the dimension of the random variable space and the 3-D sphere to a circle and a point, respectively.

In summary, the 1-D model assumes that the 10-min mean wind speed, X_1, is random but neglects the variability in the standard deviation of the wind speed, X_2, and in the 10-min maximum response, X_3. Thus, in $\boldsymbol{U}$ space, the n-dimensional "sphere" is a degenerate single point, $u_1 = \beta, u_2 = u_3 = 0$. Similarly, the 2-D model assumes that only X_1 and X_2 are random; in $\boldsymbol{U}$ space, the n-dimensional "sphere" is a degenerate circle, $u_1^2 + u_2^2 = \beta^2$; $u_3 = 0$. The 3-D model treats all three variables as random and is represented by the 3-D sphere, $u_1^2 + u_2^2 + u_3^2 = \beta^2$. Geometric representations for the three models are shown in Fig. 1. Because our target reliability is specified in terms of a return period (equal to T years) associated with the nominal load, L_{nom}, and since X_3 is defined as the extreme value in ten minutes, we need to determine the appropriate value of β to be used in the inverse-FORM approach described by the 1-D, 2-D, and 3-D models. This is done by setting $\beta =$

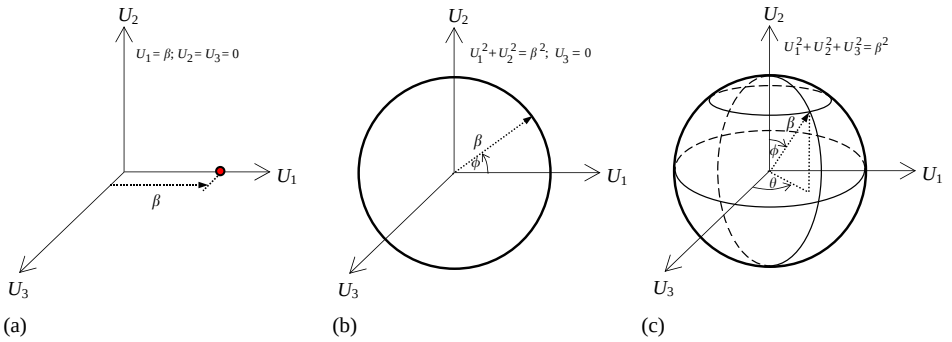

Fig. 1. Geometric representation of the n-dimensional "sphere" in $\boldsymbol{U}$ space associated with a prescribed reliability index, β, for three cases: (a) 1-D model ($n = 1$); (b) 2-D model ($n = 2$); and (c) 3-D model ($n = 3$).

$\Phi^{-1}(1 - P_f)$ where β and P_f are related to the target return period (T years) and the number of ten-minute segments in T years. Assuming stationarity of the wind speed time series over a duration of 10 min as well as independence between extremes in the various 10-min segments, the probability levels associated with any specified return period may be calculated by using the number of the 10-min segments that make up that time interval, say 20 years. This implies reference to fractiles of the distribution of the individual 10-min extreme events that is somewhat different from common practice where the return period event is defined directly in terms of the *annual* extreme event. However, the definition employed here is consistent in a similar fashion with the philosophy of the return period event. For the three return periods studied here corresponding to 1, 20, and 50 years, the values of P_f based on the aforementioned return period concept are 1.90×10^{-5}, 9.51×10^{-7}, and 3.81×10^{-7}, respectively, and the corresponding values of β are 4.12, 4.76, and 4.95, respectively.

4. Numerical studies

The wind turbine considered in this study is a 600 kW stall-regulated horizontal-axis turbine with three 21.5 m long rotor blades and a hub height of 44 m. This turbine has been the subject of previous studies and is one for which field data as well as extrapolated design loads have been derived by Ronold and Larsen [7]. The probabilistic models for the short-term maximum flapwise bending load and the environmental variables are used here with slight changes in some parameters.

In the following, we briefly discuss the derived probabilistic models for the random variables here. For more details related to the models and assumptions regarding the distributions, the reader is referred to the work of Ronold and Larsen [7]. As stated earlier, in the design for wind turbines it is typical to assume that the

extreme blade bending load may be characterized by two gross inflow parameters usually taken to be the 10-minute mean wind speed at the hub height, X_1, and the fluctuations around this mean wind speed represented by the standard deviation, X_2 of the same wind speed process. To arrive at ultimate blade bending loads under normal operating conditions, Ronold and Larsen [7] suggest representing the distribution of the 10-min mean wind speed, X_1, by a Weibull distribution whose upper tail is truncated at the cut-out speed, u_c (of 25 m/s). This implies that the present study is limited to situations where the turbine is in operating condition always. This distribution for X_1 and its parameters are illustrated in Table 1. For this example, we assume that the wind turbine is located at a site where the distribution of X_1 has a scale parameter, A, equal to 6.77 m/s (corresponding to a mean value of 6 m/s) and a shape parameter, k, of 2 (the distribution then becomes a truncated Rayleigh). The other inflow parameter describing the gross environment is taken here to be the standard deviation, X_2, of the wind speed conditional on the ten-minute mean wind speed, X_1. This second inflow parameter may be represented reasonably well by a lognormal distribution whose parameters, b_0 and b_1, both functions of X_1, and obtained based on experimental measurements, are presented in Table1.

In addition to the two inflow parameters (X_1 and X_2), the turbine response is characterized by the 10-min extreme flapwise bending moment, X_3, conditional on X_1 and X_2. The distribution of this random variable is obtained on the assumption that the underlying non-Gaussian bending moment process, $W(t)$, may be characterized by its four statistical moments (i.e., mean, μ_W; standard deviation, σ_W; skewness, α_{3W}; and kurtosis, α_{4W}) and that this non-Gaussian process (and its extremes, X_3) may be mapped to a related Gaussian process, $U(t)$, (and its own extremes, Y_3) using a four-moment Hermite transformation model [10]. Based on field data (see [7]), the first two statistical moments (μ_W and σ_W) and the zero-upcrossing rate, ν_W, of the flapwise moment, $W(t)$, are represented as functions of X_1 and X_2 as shown in Fig. 2 while the skewness, α_{3W}; and kurtosis, α_{4W} are modeled as constant values equal to -0.0066 and 2.8174, respectively. For α_{4W} less than 3, a four-moment Hermite transformation can be used to relate a Gaussian process, $U(t)$, to the physical non-Gaussian process, $W(t)$, by expanding $U(t)$ in terms of Hermite polynomials in $W_0(t)$ and Hermite moments, h_3 and h_4.

$$U(t) = W_0(t) - \sum_{n=1}^{4} h_n H_{n-1}(W_0(t)), \tag{4}$$

where $W_0(t) = (W(t) - \mu_w)/\sigma_w$ and h_n is the nth Hermite moment. Here, $h_1 = h_2 = 0$ since $W_0(t)$ has zero mean and unit variance. Also, $H_n(\ )$ is the nth Hermite polynomial. Hence, we can write Eq. (4) as follows:

$$\begin{aligned} U(t) &= W_0(t) - h_3 H_2(W_0(t)) - h_4 H_3(W_0(t)) \\ &= W_0(t) - h_3\left(W_0^2(t) - 1\right) - h_4\left(W_0^3(t) - 3W_0(t)\right) \end{aligned} \tag{5}$$

Table 1
Distributions and parameters for the random variables

Random Variable	Distribution		Parameters (adapted from Ronold and Larsen, 2000)
X_1 (wind speed)	Truncated Rayleigh	$F_{X_1}(x_1) = \dfrac{1-\exp[-(x_1/A)^k]}{1-\exp[-(u_c/A)^k]}$	$A = 6.77$ m/s, $k = 2$, $u_c = 25$ m/s
$X_2\|X_1$ (std. dev. of wind speed)	Lognormal	$F_{X_2\|X_1}(x_2) = \Phi\left(\dfrac{\ln x_2 - b_0(x_1)}{b_1(x_1)}\right)$	$b_0(x_1) = \mu_{\ln X_2\|X_1}(x_1) = -2.1601 + 1.0326 \ln x_1$
			$b_1(x_1) = \sigma_{\ln X_2\|X_1}(x_1) = 0.0579 + 0.6169 \exp(-0.1709 x_1)$
			$\mu_{X_2\|X_1}(x_1) = \exp\left[b_0(x_1) + 0.5 b_1(x_1)^2\right]$ (m/s)
			$\sigma^2_{X_2\|X_1}(x_1) = \exp\left[2b_0(x_1) + b_1(x_1)^2\right] \cdot \left[\exp\left(b_1(x_1)^2\right) - 1\right]\left(\text{m/s}\right)^2$
$X_3\|X_1, X_2$ (extreme flap bending moment in ten minutes)	Hermite model based on four moments	See Eqs. (6) and (7) for details.	$\mu_W = \mu_W(x_1), \sigma_W = \sigma_W(x_1, x_2)$, and $v_W = v_W(x_1)$ are shown in Fig. 2.
			$\alpha_{3W} = -0.0066$
			$\alpha_{4W} = -0.0066$

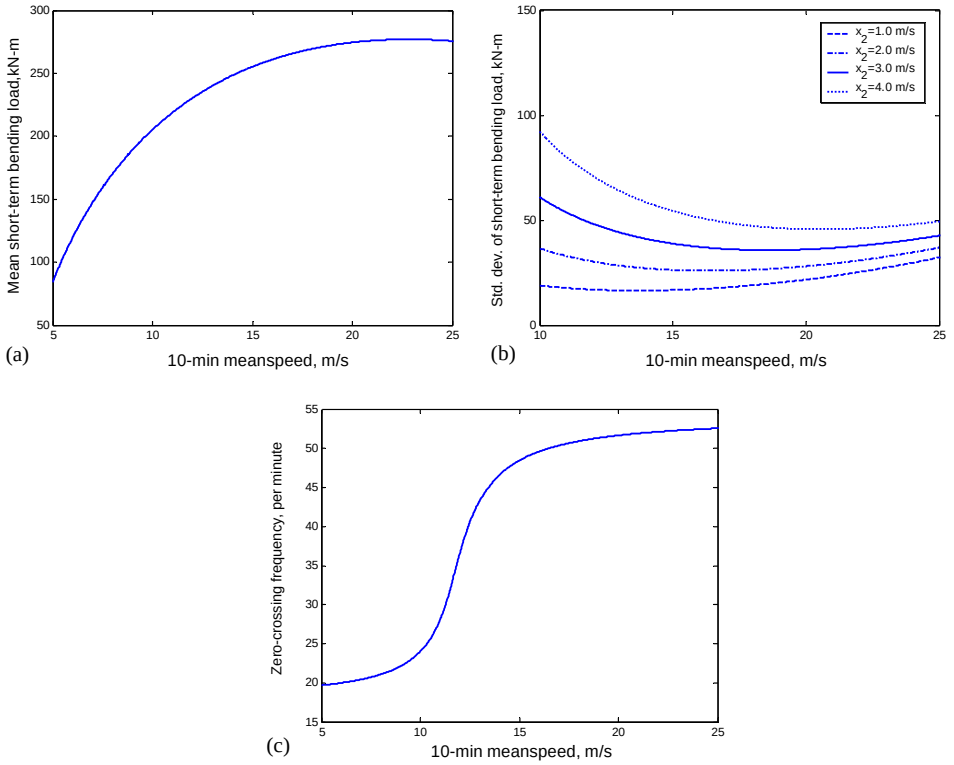

Fig. 2. Dependence on mean wind speed (X_1) of short-term maximum bending load model parameters: (a) mean value, μ_W; (b) standard deviation, σ_W; and (c) zero-crossing frequency, ν_W.

One can also rewrite Eq. (5) by expressing $W(t)$ in terms of $U(t)$:

$$W(t) = f(U(t)) = \mu_W + \sigma_W \left[\left(\sqrt{c(t)^2 + k} + c(t) \right)^{1/3} - \left(\sqrt{c^2 + k} - c(t) \right)^{1/3} - a \right],$$

$$h_3 = \frac{\alpha_{3W}}{6}, \quad h_4 = \frac{\alpha_{4W} - 3}{24},$$

$$a = \frac{h_3}{3h_4}, \quad b = -\frac{1}{3h_4}, \quad k = (b - 1 - a^2)^3,$$

$$c(t) = 1.5b(a + U(t)) - a^3. \tag{6}$$

Note that the mapping from U to W as expressed by the transformation in Eq. (6) remains monotonic as long as $\mathrm{d}U/\mathrm{d}W > 0$, or equivalently as long as $16\alpha_{3W}^2 < 9(3 - \alpha_{4W})(5 + \alpha_{4W})$ (see [11] for details). This inequality is satisfied for our problem since we have $\alpha_{3W} = -0.0066$ and $\alpha_{4W} = 2.8174$ here. Note also that Eq. (5) should actually use two different undetermined coefficients (say $\tilde{h}_3$ and $\tilde{h}_4$) than h_3 and h_4 but to first order (i.e., ignoring product terms such as $\tilde{h}_3\tilde{h}_4$), those coefficients have been solved for by Winterstein [10] and shown to be the same as the Hermite

moments, h_3 and h_4. Improvements to these coefficients are possible by retaining terms of higher order. To determine the distribution of the extreme, X_3, of the flapwise bending moment process, $W(t)$, it is necessary to relate X_3 to Y_3, the extreme of the Gaussian process, $U(t)$, where the distribution of Y_3 may be given as follows:

$$F_{Y_3}(u) = \exp\left[-\nu_W T \exp\left(-\frac{u^2}{2}\right)\right]. \tag{7}$$

Once the distribution for Y_3 is known, the distribution for X_3 may be found using the Hermite transformation model given by Eq. (6), i.e., $X_3 = f(Y_3)$. Note that dependence of X_3 on X_1 and X_2 is implicit in the formulation above.

4.1. 1-D model

Here, only the 10-min mean wind speed, X_1, is modeled as random, while the standard deviation of wind speed, X_2, and the 10-min maximum response, X_3, are held at their (conditional) median levels. Knowing the reliability index, β, associated with a prescribed return period and failure probability, one can immediately obtain the "point" corresponding to that failure probability in the standard normal ($\boldsymbol{U}$) space (see Fig. 1a) as follows:

$$u_1 = \beta,\ u_2 = 0,\ \text{and}\ u_3 = 0. \tag{8}$$

The design point related to the nominal bending load in physical random variable space ($\boldsymbol{X}$) may be obtained using the Rosenblatt transformation:

$$x_1 = F_{X_1}^{-1}[\Phi(\beta)],\ x_2 = F_{X_2|X_1}^{-1}[\Phi(0)],\ \text{and}\ x_3 = F_{X_3|X_1,X_2}^{-1}[\Phi(0)]. \tag{9}$$

From Eq. (9), it is clear that median values of X_2 and X_3 lead to the nominal loads. This is illustrated graphically in Fig. 3, where, for example, the 20-year design load is seen to be 420.8 kN m which is derived using a mean wind speed of 24.5 m/s and a standard deviation of wind speed equal to 3.13 m/s. Similar results for the other return periods are also shown. Detailed results for all three return periods are summarized in Table 2.

4.2. 2-D model

Randomness in both of the environmental variables, X_1 and X_2, is now modeled while the load variable, X_3, is still assumed deterministic at its (conditional) median level. For a known reliability index, β, one can construct a "circle" in standard normal ($\boldsymbol{U}$) space (see Fig. 1b) as follows:

$$u_1 = \beta\cos\phi,\ u_2 = \beta\sin\phi, \quad \text{and} \quad u_3 = 0, \quad \text{for} -\pi \leqslant \phi \leqslant \pi. \tag{10}$$

Since this circle lies in the plane, $u_3 = 0$, it is associated only with the environmental random variables and hence it is termed an "environmental contour." To obtain the design point, one needs to search the entire circle (by considering all values of the angle ϕ between $-\pi$ and π) so as to find the largest median response

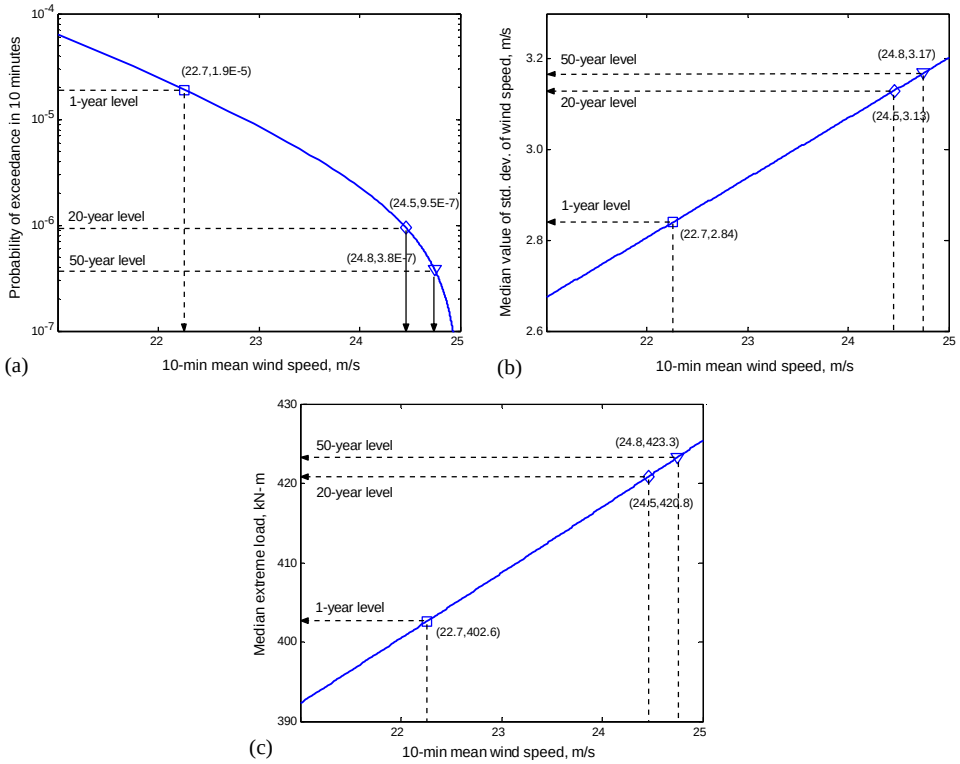

Fig. 3. Procedure to estimate extreme loads based on the 1-D model: (a) evaluating X_1 for a specified return period; (b) evaluating $\hat{X}_2$ given X_1; and (c) evaluating $\hat{X}_3$ given X_1 and $\hat{X}_2$.

Table 2
Results summarizing design points from the 1-D, 2-D, and 3-D models for three return periods

Return Period (yr)	1-D			2-D			3-D		
	X_1 (m/s)	X_2 (m/s)	X_3 (kN m)	X_1 (m/s)	X_2 (m/s)	X_3 (kN m)	X_1 (m/s)	X_2 (m/s)	X_3 (kN m)
1	22.7	2.84	402.6	22.0	2.95	404.2	21.3	2.83	410.5
20	24.5	3.13	420.8	24.1	3.33	423.8	23.1	3.12	436.8
50	24.8	3.17	423.3	24.4	3.44	427.7	23.5	3.17	444.0

value for X_3. Applying the Rosenblatt transformation yields the design point in $\boldsymbol{X}$ space:

$$x_1 = F_{X_1}^{-1}[\Phi(\beta\cos\phi)],\ x_2 = F_{X_2|X_1}^{-1}[\Phi(\beta\sin\phi)],\ \text{and}\ x_3 = F_{X_3|X_1,X_2}^{-1}[\Phi(0)]. \quad (11)$$

Every point on the environmental contour is such that the probability on the side of a tangent hyperplane at that point (away from the origin) is the same. However, each point is associated with a different "median" response. As shown in Fig. 4, for a

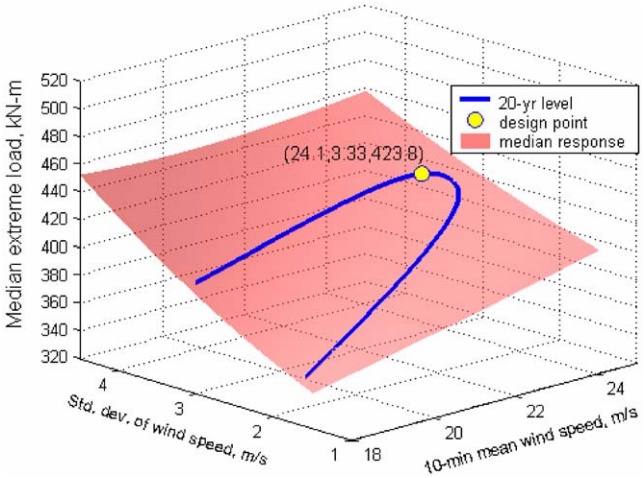

Fig. 4. Median response surface, 20-year environmental contour, and design point.

20-year return period, Eq. (11) maps the contour in $\boldsymbol{U}$ space to different median levels of response, whose maximum value is 423.8 kN m which is associated with a mean wind speed of 24.1 m/s and a standard deviation of wind speed equal to 3.33 m/s. The nominal bending load for this 2-D model can also be obtained by plotting separate iso-response curves of median values of X_3 together with the 2-D environmental contour in $\boldsymbol{X}$ space and locating the iso-response curve of highest value that intersects the 2-D environmental contour. It should be noted that the environmental contours and the iso-response curves may be constructed independently; hence, these contours are not turbine-specific. The turbine response/load is uncoupled from the environment. Environmental contours as well as iso-response curves are plotted in Fig. 5 from which it may be seen that the nominal loads are 404.2, 423.8, and 427.7 kN m, respectively, for 1-, 20-, and 50-year return periods. Detailed results for all three return periods are summarized in Table 2.

4.3. 3-D model

Randomness in all three random variables, X_1, X_2, and X_3 is now modeled. For a known reliability index, β, one can construct a sphere in standard normal ($\boldsymbol{U}$) space (see Fig. 1c) as follows:

$$u_1 = \beta \sin\phi \sin\theta,\ u_2 = \beta\cos\phi, \quad \text{and} \quad u_3 = \beta \sin\phi\cos\theta, \quad \text{for} -\pi \leqslant \phi \leqslant \pi, \quad 0 \leqslant \theta \leqslant \pi. \tag{12}$$

To obtain the design point, one needs to search the entire sphere (by considering all values of the angle ϕ and θ) so as to find the largest response value for X_3. Applying the Rosenblatt transformation yields the design point

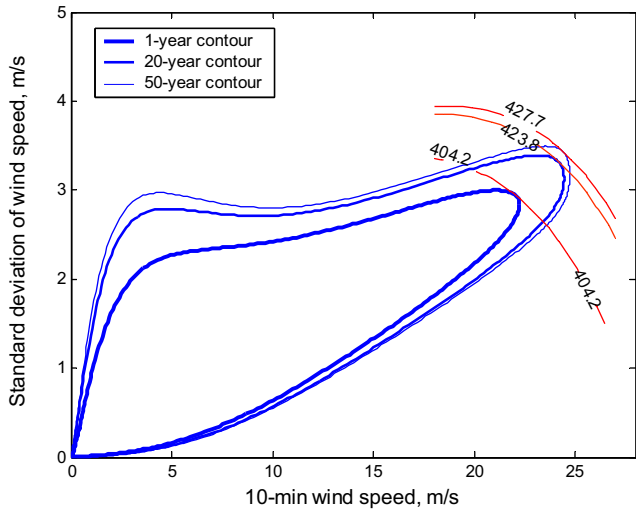

Fig. 5. Environmental contours for different return periods and iso-response curves.

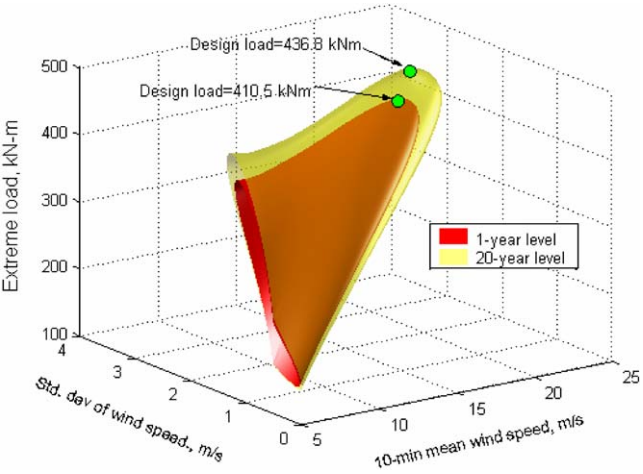

Fig. 6. 3-D surfaces employed for deriving 1- and 20-year nominal loads with the 3-D model.

in $\boldsymbol{X}$ space:

$$x_1 = F_{X_1}^{-1}[\Phi(\beta \sin\phi \sin\theta)],\ x_2 = F_{X_2|X_1}^{-1}[\Phi(\beta \cos\phi)],\quad \text{and}$$
$$x_3 = F_{X_3|X_1,X_2}^{-1}[\Phi(\beta \sin\phi \cos\theta)]. \tag{13}$$

As shown in Fig. 6, for a 20-year return period, Eq. (13) maps the sphere in $\boldsymbol{U}$ space to different levels of response, X_3—the maximum value of response is found to be

Table 3
Modified 2-D model results for three return periods

Return Period (yr)	Direction cosine, α_3	Modified fractile for U_3	X_3 (kN m)
1	0.26	0.71	409.9
20	0.45	0.87	437.7
50	0.51	0.91	445.5

436.8 kN m; for the 1-year return period, this maximum response is 410.5 kN m. Detailed results for all three return periods are summarized in Table 2.

4.4. Discussions and a proposed modified 2-D model

The three models presented above lead to different nominal loads as is seen in Table 2. In the table, it is seen that as would be expected, the nominal load levels increase with return period. For any return period, it is seen that the 1-D and 2-D models yield very slightly different loads; this is because the variable, X_2, the standard deviation of wind speed, is relatively unimportant compared to the mean wind speed, X_1. For the 20-year return period, the difference in nominal loads is only about 0.7%. Greater differences are seen when the 3-D model is considered where short-term response uncertainty is included. The 3-D model 20-year loads are about 3% higher than the 2-D loads. While for this particular problem, the difference between the 3-D model and the simpler models is small, this may not be the case when response variability (conditional on inflow) is large.

The 2-D model is of special interest because it uncouples the environment from the response. This is especially convenient when considering the same turbine in different environment conditions as well as when considering alternative turbines for a specified environment. Moreover, a modified 2-D model that employs omission factors (Madsen, 1988) to derive higher-than-median fractiles of U_3 (and hence X_3) can, with few additional calculations that follow a 2-D model analysis, reduce the error relative to the 3-D model. Results from such a 2-D modified model are summarized in Table 3 where the FORM direction cosine, α_3, which is related to the importance of the response variable, was obtained by only computing a local gradient of the limit state function in the direction of U_3 (at the 2-D model design point). Fig. 7 shows nominal load levels from all four models where it is clear that there is now negligible difference between the loads derived from the modified 2-D model and those from the 3-D model.

5. Conclusions

We have presented a procedure to establish nominal loads for the design of wind turbines against ultimate limit states. Three alternative load models (termed 1-D, 2-D, and 3-D models) were compared. An inverse reliability approach was employed

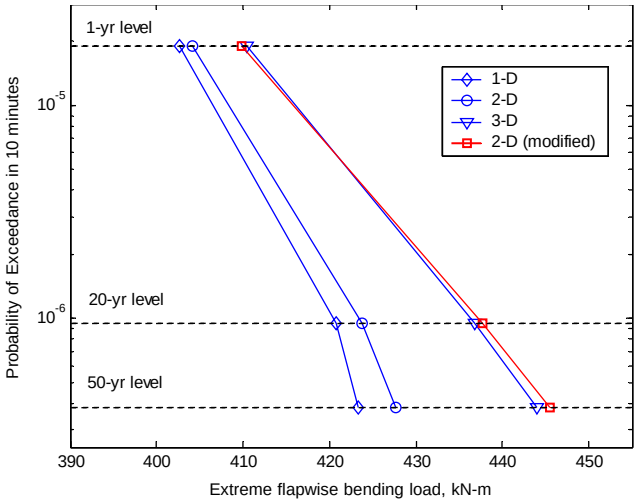

Fig. 7. Extreme flapwise bending moment for 1-, 20-, and 50-year return periods based on a 1-D, 2-D, 3-D, and a modified 2-D model.

to estimate nominal design loads. For the 600 kW wind turbine considered, the environmental and response probabilistic descriptions were obtained from a study by Ronold and Larsen [7]. Extreme flapwise bending loads were studied and, for this turbine, it was found that the difference between the nominal loads derived from 1-D and 2-D models was very small since the standard deviation of wind speed at the hub height had a very small effect on the extreme bending load compared with the mean wind speed. Including uncertainty in the short-term maximum bending load conditional on inflow (in the 3-D model) caused somewhat higher loads than in the 1-D and 2-D models. The modified 2-D model that uses higher-than-median fractiles (derived by some additional calculations following the 2-D analysis) for the short-term response conditional on inflow was able to yield almost similar nominal loads as were obtained with the 3-D model.

The results presented were for a specific wind turbine, and conclusions drawn from this study are by no means generally applicable to other wind turbines or for other environmental conditions. However, the procedures outlined may be employed in any situation where the objective is to establish nominal loads for the reliability-based design of wind turbine components.

Acknowledgements

The authors gratefully acknowledge the financial support provided by Grant No. 003658-0272-2001 awarded through the Advanced Research Program of the Texas

Higher Education Coordinating Board. They also acknowledge additional support from Sandia National Laboratories by way of Grant No. 30914.

References

[1] IEC/TC88 61400-1 ed. 2. Wind Turbine Generator Systems—Part 1: Safety Requirements, International Electrotechnical Commission (IEC), Geneva, Switzerland, 1998.
[2] H.O. Madsen, S. Krenk, N.C. Lind, Methods of Structural Safety, Prentice-Hall Inc., Englewood Cliffs, NJ, 1986.
[3] S.R. Winterstein, T.C. Ude, C.A. Cornell, P. Bjerager, S. Haver, Environmental contours for extreme response: inverse FORM with omission factors, Proceedings of the ICOSSAR-93, Innsbruck. 1993.
[4] A. Der Kiureghian, Y. Zhang, C.-C. Li, Inverse reliability problem, J. Eng. Mech. ASCE 120 (5) (1994) 1154–1159.
[5] H. Li, R.O. Foschi, An inverse reliability method and its application, Struct. Safety 20 (1998) 257–270.
[6] L.M. Fitzwater, C.A. Cornell, P.S. Veers, Using environmental contours to predict extreme events on wind turbines, Wind Energy Symposium, AIAA/ASME, 2003, pp. 244–258.
[7] K.O. Ronold, G.C. Larsen, Reliability-based design of wind-turbine rotor blades against failure in ultimate loading, Eng. Struct. 22 (2000) 565–574.
[8] H.O. Madsen, Omission sensitivity factors, Struct. Safety 5 (1988) 35–45.
[9] M. Rosenblatt, Remarks on a multivariate transformation, Ann. Math. Stat. 23 (1952) 470–472.
[10] S.R. Winterstein, Nonlinear vibration models for extremes and fatigue, J. Eng. Mech. ASCE 114 (1988) 1772–1790.
[11] S.R. Winterstein, Moment-based Hermite models of random vibration, Report No. 219, Department of Structural Engineering, Technical University of Denmark, Lyngby, Denmark, 1987.